Measurement of Charge Excitations in MgB_2 by Inelastic X-ray Scattering

The recent discovery of superconductivity in MgB_2 at a critical temperature $T_c \sim 39K$, the highest among simple binary compounds, has stimulated extensive theoretical and experimental studies worldwide. Unlike high-T_c cuprates, the relatively simple crystal structure of MgB_2 allows detailed first-principle calculations to be performed and compared with experiment. MgB_2 is now understood as a phonon-mediated conventional superconductor, i.e., the mechanism for paring involves an attractive interaction between electrons mediated by lattice vibrations, with multiple gaps facilitated by its unusual band structure. The density of states near the Fermi energy is dominated by the covalent, graphite-like B sublattice with two types of B bands: the 3D π bands connecting adjacent B layers and the 2D σ bands confined within the B layers. The presence of strong electron-phonon coupling between the flat σ bands and the in-plane vibration of the B layer (the E_{2g} phonons) dominates the superconducting properties and is largely responsible for the unusually high T_c.

Even within this phonon-mediated picture of superconductivity, dynamical screened electron-electron and electron-phonon interactions play an important role, the study of which should provide further insight into the superconducting behaviors of the material. In particular, the measurement and comparison with first-principle calculations of the dynamical density response function give detailed information on the electronic excitations that control most of the macroscopic properties, and at the same time, provide a stringent test of the theory.

In this article, we report the first measurement of the dynamical structure factor $S(q,\omega)$ of electrons in single-crystal MgB_2 using non-resonant inelastic x-ray scattering (IXS) on the Taiwan IXS beamline (BL12XU) at SPring-8. Inelastic x-ray scattering coupled with brilliant and intense 3rd generation synchrotron radiation sources provides a powerful tool for investigating lattice dynamics and correlation effects of electrons in many-electron systems. Technical advances in the last decades have made possible the construction of dedicated facilities that routinely deliver x-ray beams with focus of ~100 μm, tunable energy resolutions to meet specific experimental needs, and flux on the order of 10^{10} photons/sec/meV for IXS experiments. For the present experiment, the small focus of the x-ray beam plays a decisive role as single crystals of MgB_2 exist at present only in very small size (~0.01 mm^3). The use of hard x-rays ensures that the probed properties originate from the bulk. The stability and high performance of BL12XU also contribute to the successful measurement of the high quality data reported here.

The MgB_2 single crystals used in the present study were prepared by high-pressure sintering of MgB_2 powder by Takano *et al.,* [Appl. Phys. Lett. **78**, 2914 (2001)]. Good single crystals were plate-like, golden in color, and measure ~500×300×20 μm^3 in size (see, Fig.1 (a)). The quality and orientation of the crystals were characterized by indexing rotation photos as shown in Fig.1(b), where principal Bragg diffraction spots were identified and used to align the *c*- and *a*- (or equivalently the *b*-) axes to the horizontal scattering plane. Rocking curve widths were on the order of 0.05°. The weak powder rings indicated a small degree of texture.

The IXS measurement was carried out at room temperature using two configurations of the beamline and the IXS spectrometer with a total energy resolution of 65 and 250 meV, respectively. The momentum resolution was fixed at 0.06 $Å^{-1}$. The incident energy was scanned around 9.886 keV, which corresponded to the near backscattering

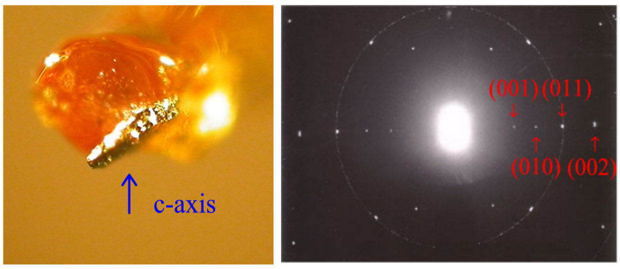

***Fig. 1:** Photo of a typical MgB_2 single crystal used in the experiment and its rotation photo. In the example shown, the c- and a- (or equivalently the b-) axes have been aligned to the horizontal plane. Notice that the c-axis is not (necessarily) perpendicular to the plate surface. The weak powder rings indicate a small degree of texture.*

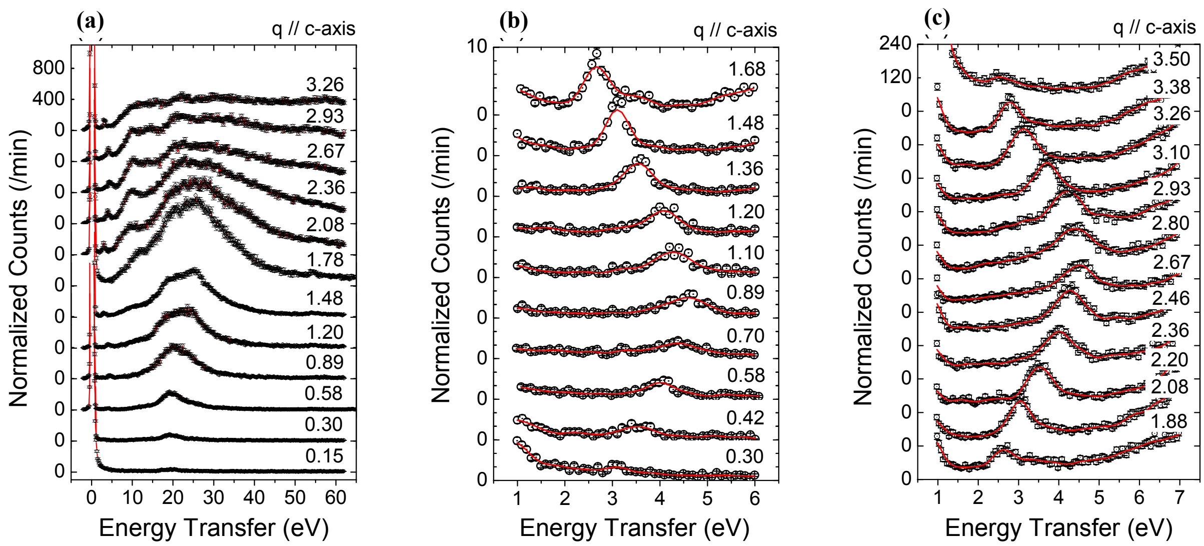

***Fig. 2:** Inelastic x-ray scattering spectra of MgB_2 taken at room temperature along the c-axis at various momentum transfers q ($Å^{-1}$). Spectra taken over energy transfers of 0 - 60 eV and momentum transfers covering the size of two Brillouin zones in the ΓA direction are shown in (a). Spectra taken with finer energy steps over the energy tranfer region of 1 - 7 eV for the prominent low energy feature in the first and second periods are shown in (b) and (c), respectively. The total energy resolution was 250 (or 65) meV for spectra shown in (a) and (c) (or (b)).*

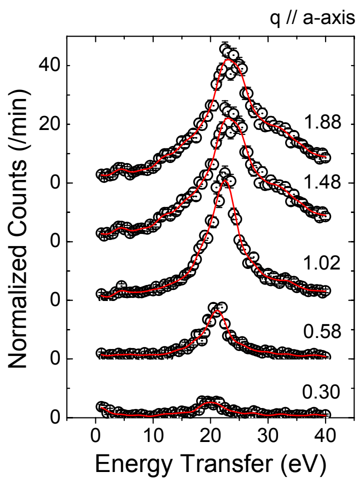

***Fig. 3:** Inelastic x-ray scattering spectra of MgB_2 taken at room temperature along the a-axis at various momentum transfers q ($Å^{-1}$). The momentum transfers cover one Brillouin zone size in the ΓM direction. The total energy resolution was 65 meV.*

reflection energy of the Si(555) spherical analyzer used on the spectrometer. Data taken with momentum transfer q along the c- and a-axes were summarized in Fig. 2, and Fig. 3, respectively. In the following, a brief analysis and discussion of the data are given. A full analysis will be published elsewhere.

So far, two groups have carried out first-principle calculations of the density response function of MgB_2. Zhukov *et al.* [Phys. Rev. B **64**, 180507 R (2001)] used both the plane-wave pseudopotential and the tight-binding LMTO methods, whereas Ku *et al.* [Phys. Rev. Lett. **88**, 057001 (2002)] based their calculation on the time-dependent density functional theory. From the calculated density response function $\chi(\mathrm{q},\omega)$, the dielectric function $\varepsilon(\mathrm{q},\omega)$ can be obtained through $\varepsilon=[1+(4\pi e^2/q^2)\chi]^{-1}$, and the fluctuation-dissipation theorem provides the connection of these macroscopic properties with the measured dynamical structure factor $S(\mathrm{q},\omega)$:

$$S(\mathrm{q},\omega)=-\frac{\hbar q^2}{4\pi^2 e^2 n}\mathrm{Im}\,\varepsilon^{-1}(\mathrm{q},\omega)=-\frac{\hbar}{\pi n}\mathrm{Im}\,\chi(\mathrm{q},\omega).$$

The results of both calculations showed that, in addition to the free-electron-like bulk plasmon mode (defined as $\mathrm{Re}\varepsilon=0$ and $\mathrm{Im}\varepsilon<<1$, which lead to a pronounced maximum in the energy loss function $-\mathrm{Im}\,\varepsilon^{-1}(q,\omega)$) at ω of 18 – 22 eV, there was a sharp collective charge excitation of practically zero width between 2 – 5 eV with q parallel to the c-axis. This feature was found by Ku *et al.* to be associated with the 5 eV strong absorption feature in $\mathrm{Im}\varepsilon$ induced by interband transitions between the in-plane parallel bands of the occupied B π-bands and unoccupied Mg states of σ symmetry, and was therefore interpreted as arising from coherent charge fluctuations between the Mg and B layers. The feature dispersed weakly with q and decayed into the single-particle continuum at q ~ 0.6 $Å^{-1}$. For q parallel to the a-axis, no similar collective excitation was predicted by Ku *et al.* over the same low-energy region, whereas Zhukov *et al.* found that a collective and broader excitation exists for q in the in-plane directions between 2 – 8 eV. A couple of other features in the same energy region caused by interband transitions were also reported. Zhukov *et al* furthermore studied the hypothetical B_2 crystal and found similar low-energy collective excitations arising from charge fluctuations between the in-plane parallel π and σ boron bands; the energies were however ~2 eV higher due to the weaker interaction between the B layers in B_2. All these calculations were carried out only for q values within the first Brillouin zone.

As far as the free-electron-like bulk plasmon at 18 – 22 eV is concerned, our data shown in Fig. 2(a) and 3 match well with both calculations in energy and dispersion for momentum transfers along the c- and a-axes up to the 1st Brillouin zone boundary, beyond which single-particle excitations begin to dominate in the energy region, particularly for q along the c-axis. The detailed lineshape published by Zhukov *et al.*, however, show more structures than our data.

For q along the c-axis, a periodic and prominent feature at energy transfer of 2 – 5 eV was observed (see Fig. 2) throughout the q values investigated. Similar low-energy features were not observed for q along the a-axis. We have determined the energy position and width by fitting a Gaussian and a linear slope function to the feature. The results are summarized in Fig. 4. The most remarkable of the observed energy dispersion of the feature is that the dispersion can be described entirely by a simple cosine function of the form (the cosine fit curve in Fig. 4(a)):

$$\omega = \omega_0 - 2\gamma\cos(qc) \,,$$

where $\omega_0 = 3.55$ eV, $\gamma = 0.49$ eV, and $c = 3.52$ Å the lattice constant of MgB_2 along the c-axis. The width of the feature, which is ~0.5 eV near Γ and ~1 eV near A, also displays periodicity (Fig. 4(b)). The observed energy and width dispersion of the feature are independent of the energy resolution used.

Naturally it is tempting to associate this low-energy excitation feature with the sharp collective mode at $q \leq 0.6$ Å^{-1} along the c-axis predicted by the aforementioned first-principle calculations. There are, however, some difficulties in making the association. Firstly, there is the apparent discrepancy in the energy dispersion and the width of the observed feature as compared to the theoretical predictions. Secondly, the predicted collective mode was shown by Ku *et al.* to decay into single-particle intraband excitations of the occupied B π-bands in ΓA at $q \sim 0.6$ Å^{-1}, whereas the observed feature shows periodic dispersion over the entire q range investigated, and persists even when the bulk plasmon feature at ~20 eV has decayed into the single-particle continuum. One may suggest that the observed feature at $q > 0.6$ Å^{-1} may be linked with the single-particle intraband excitations of the occupied B π-bands controlled by Imε in the calculation. This is, however, quite unlikely as the single-particle continuum seen at $q > 1.78$ Å^{-1} at energies above 10 eV in Fig. 2 shows no evidence of any periodic structure, particularly considering that the 10-eV feature in Fig. 2 may originate from the 5-eV optical interband transitions in Imε from the same calculation. This feature in Imε disperses from ~5 eV at $q = 0$ to ~10 eV near the zone boundary with reducing strength and broadening, behaving in a similar way as the intraband excitations of the B π-bands mentioned above. Examination of the MgB_2 band structure also fails to

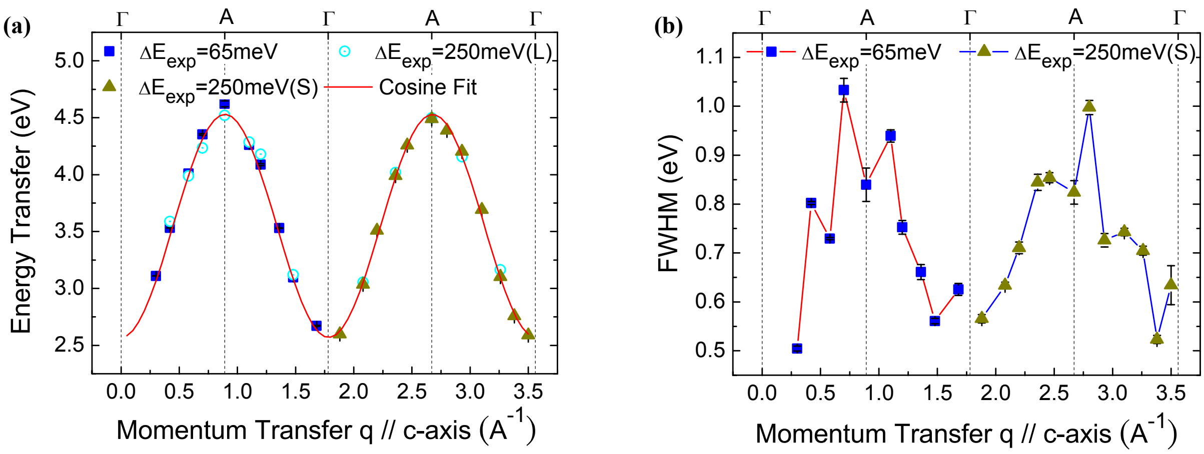

***Fig. 4:** Periodic energy and width (FWHM) dispersion of the prominent excitation feature at 2.5 - 4.5 eV along the c-axis observed in the data shown in Fig. 2. The open circles (labeled L) are obtained from the wide energy scans shown in Fig. 2(a), from which only the peak position was extracted from the fit.*

suggest other possible interband transitions mediated by the momentum transfers at the excitation energy (transfer) of the observed periodic feature. One cannot therefore explain the observed periodic feature as a combination of the predicted low-energy collective charge excitations at low q and single-particle excitations at high q from the occupied B π-bands.

From our data and existing calculations alone, it is not possible to clearly establish the mechanism of the observed periodic and prominent charge excitation observed along the c-axis in MgB_2. One plausible scenario, hinted by the cosine energy dispersion of the feature, is that it may be caused by the formation of bound electron-hole pairs involving holes from the 2D σ bands and electrons from the 3D π bands of the B lattice due to dynamical exchange-correlation effects of the charge carriers. One important evidence for this connection is that, at $q = 0$, the energy of this feature 2.57 eV as determined from the dispersion curve corresponds to the energy of the occupied B π-bands at Γ, whereas the effective mass, $m^* = \hbar^2/(2\gamma c^2) = (13.6/\gamma)(a_0/c)^2 m = 0.62m$, is nearly the same as the band mass of the hole carriers of the B σ-bands. It is hoped that the data presented here will prompt further theoretical studies, leading to better understanding of the dynamical response of electrons in MgB_2 as well as possible link of the observed low-energy charge excitations with the high T_c superconductivity. Realistic first-principle calculations of the dynamical response function taking into account dynamical exchange-correlation effects and influence of the crystal local field at short wavelength may be needed.

BEAMLINE
SP12U Inelastic X-ray Scattering beamline

EXPERIMENTAL STATION
IXS Spectrometer end station

AUTHORS
Y. Q. Cai, P. Chow, H. Ishii, C. C. Chen,
K. S. Liang, and C. T. Chen
National Synchrotron Radiation Research Center,
Hsinchu, Taiwan

PUBLICATIONS

- Y. Q. Cai, C. C. Chen, P. Chow, K. L. Tsang, C. T. Chen, and C. C. Kao, SRRC Activity Report 2001/2002, 83 (2002).
- Y. Q. Cai, P. Chow, H. Ishii, D. J. Wang, and C. T. Chen, NSRRC Activity Report 2002/2003, 99 (2003).
- Y. Q. Cai, P. Chow, H. Ishii, C. C. Chen, K.S. Liang, C. T. Chen, S. Tsuda, S. Shin, Y. Takano, H. Kito, and C. C. Kao (in preparation).

CONTACT E-MAIL
cai@nsrrc.org.tw